

28 May 2010, 2:00 pm - 3:30 pm

# Floatation of Tunnel in Liquefiable Soil

S. C. Chian
*University of Cambridge, U. K.*

S. P. G. Madabhushi
*University of Cambridge, U. K.*


Fifth International Conference on
Recent Advances in Geotechnical Earthquake Engineering and Soil Dynamics
*and Symposium in Honor of Professor I.M. Idriss*
May 24-29, 2010 • San Diego, California

# FLOATATION OF TUNNEL IN LIQUEFIABLE SOIL

**S.C. Chian**
University of Cambridge
Cambridge CB3 0EL, UK

**S.P.G. Madabhushi**
University of Cambridge
Cambridge CB3 0EL, UK

ABSTRACT

Underground structures such as tunnels have a lower unit weight than the surrounding soil and are commonly deemed to be susceptible to floatation in liquefiable soil. In the process of floatation, the tunnel has to possess ample buoyancy force to shear and carry the overlying soil upwards. This is aided by soil liquefaction resulting from the increase in water pressure with number of earthquake loading cycles. With onset of liquefaction, effective stress decreases which lead to a reduction in the shear strength of soil, hence assisting the floatation of tunnel. Conversely, the total stress exerted by the overburden soil suppresses the process. A series of centrifuge tests were conducted to investigate the floatation of tunnels in liquefiable sand deposits. This paper discusses the initiation and cessation of the floatation as well as the floatation susceptibility of varying depths of tunnels.

## INTRODUCTION

Underground infrastructure has been a widespread alternative in redeveloping urban spaces to ease congestion pressure arising from land scarcity. These underground structures often offer separation of conflicting activities and enjoy less-constrained development space accompanied with other benefits such as protection and discretion from the public. Hence, they have often been served as vital lifelines facilities for transport, utility and storage purposes. They include subway train tunnels, gas and water pipelines, car parks, goods warehouses and fuel storage tanks. However, in the event of earthquakes, the functionality of these lifelines could be put in question especially in soils susceptible to liquefaction.

Historical earthquake events such as the 1964 Niigata earthquake (Seed, 1970), 1964 Alaska earthquake (Hall and O'Rourke, 1991), 1906 San Francisco earthquake (Youd and Hoose, 1976) and the 1994 Northridge earthquake (Bardet and Davis, 1999) have proven the damage susceptibility of underground structures including large buried pipelines and tanks. Damage to buried lifelines such as utilities (power, water, gas), communication networks, and transportation systems by earthquakes can create dangerous situations. Broken gas and power lines are serious threats to safety because of fire risk as witnessed during the Kobe earthquake of 1995 (Bardet et al, 1995) and Northridge earthquake of 1994 (EERI, 1994 and 1995) where cracked water mains reduced the amount of water available for fire suppression. Similarly, blocked or damaged transportation routes interfere with the ability of emergency personnel to respond promptly to immediate crisis.

During liquefaction, the shear strength of a saturated cohesionless soil is reduced dramatically due to increase in pore water pressure. Therefore it is logical to expect that tunnels and other underground lifelines would float due to their buoyancy as portrayed in past earthquakes. More underground structures have been constructed during the past couple of decades than before. Such failure of underground structures poses risks of high human casualties and property losses which has been a growing concern with tunnels proposed and constructed in active seismic areas worldwide. Existing major tunnels built in earthquake-prone areas include the George Massey highway tunnel in Vancouver (Canada) and the San Francisco's Bay Area Rapid Transit (BART). Other seismic active regions are also in the midst of constructing significant lengths of tunnels in liquefiable soils such as the Thessaloniki Highway Tunnel and Marmaray Rail Tunnel in Greece and Turkey respectively. Each of these underground infrastructures carries thousands of commuters during peak hours and evidently poses extreme concerns to public safety in events of strong earthquake.

A centrifuge testing program was conducted in Schofield Centre at the University of Cambridge to investigate floatation of large prototype tunnels of 5m diameter. This paper seeks to provide an understanding of such floatation failures.

METHODOLOGY

Centrifuge Modelling

Soil is a highly non-linear material. It is therefore essential to replicate identical stress and strain conditions as in the prototype scale in laboratory tests. Geotechnical centrifuge modelling achieves these conditions with the use of high centrifugal acceleration to scale up the model. With reference to Fig. 1, a scaled model is made to correspond with the prototype at the pre-determined centrifuge g-level. As a result, a 1:*N* model experiences the same stress-strain condition as the prototype when subjected to a centrifugal acceleration of *N* x g level (Schofield, 1980). A set of scaling laws were derived so as to interpret other centrifuge testing parameters in prototype scale. They are described in Table 1.

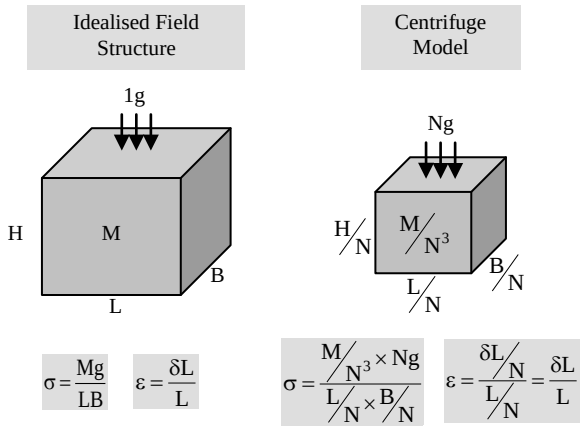


*Fig. 1. Identical stress-strain condition between model and prototype*

Table 1. Centrifuge scaling laws

| Parameter | Model/Prototype | Dimensions |
|---|---|---|
| Length | 1/N | L |
| Acceleration | N | $LT^{-2}$ |
| Velocity | 1 | $LT^{-1}$ |
| Strain | 1 | 1 |
| Stress | 1 | $ML^{-1}T^{-2}$ |
| Force | $1/N^2$ | $MLT^{-2}$ |
| Mass | $1/N^3$ | M |
| Seepage Velocity | N | $LT^{-1}$ |
| Time (Seepage) | $1/N^2$ | T |
| Time (Dynamic) | 1/N | T |

Table 1 indicates that there is a conflict in the time scaling between the dynamic and consolidation events. High viscous pore fluid was used in the dynamic centrifuge test so as to overcome this inconsistency.

Equipment

The beam centrifuge in Cambridge measures 10 metres in diameter with a maximum g-level of 100g for dynamic tests. The swinging platforms at each end of the arm are pivoted and designed to hold payloads of up to 1 tonne. One arm of the centrifuge swing holds the model and experimental equipment whilst the opposite arm carrying a counterweight. When the centrifuge accelerates, both arms swing up to the horizontal plane simultaneously. Specific design and operation of the beam centrifuge are provided in Schofield (1980, 1981).

The Stored Angular Momentum (SAM) earthquake actuator devised by Madabhushi et al (1998) is capable of applying strong lateral motions to the centrifuge package up to 0.3g PGA in a 100g test. Sufficient energy is stored in the actuator in a 3-phase motor in a pair of rotating flywheels attached to two balanced reciprocating rods. Strong earthquake is then fired by closing a fast-acting hydraulic clutch with one of the rods passing through the clutch. This reciprocating motion rotates the shaft with an offsetting variable length lever arm which converts the motion into horizontal shaking of the centrifuge package. The magnitude of the earthquake is controlled by adjusting the offset distance with the variable length of the lever arm. The frequency is determined by altering the rotational speed of the flywheels. In addition, the time duration of the shaking corresponds to the duration of the clutch closure adjusted using an electronic timer connected to the beam centrifuge.

The automatic sand pourer was commissioned in 2006 and relied on the concept of sand pluviation by gravity. The relative density of the sand can be adjusted by varying the flow rate and drop height of the nozzle to the desired pour location within the model boxes. Details of design and capabilities of the sand pourer were established by Madabhushi et al (2006) and Zhao et al (2006). The suitability of the apparatus in producing loose liquefiable sand samples was described by Chian et al (2009).

The saturation system (CAM-Sat) was recently developed by Stringer and Madabhushi (2009). The model box is driven under vacuum while fluid flows from a tank into it via 4 inlet pipes. The Cam-Sat system, running with a programmable software platform called DASYLAB, relies on the real-time monitoring of the fluid flow rate derived from the change in weight to adjust the optimum pressure difference between the feeding tank and the model box.

Instrumentation

Instruments such as accelerometers, pore pressure transducers and potentiometers were used in the centrifuge test. The accelerometers (ACC) rely on the acceleration/charge conversion accomplished by means of a shear couple applied to a piezoceramic plate or tube. The pore pressure transducers (PPT) measure hydrostatic pore pressures at specific locations in the models throughout the centrifuge test. Each of the

transducers measures the fluid pressure exerted onto a flexible diaphragm in the instrument. Draw-wire potentiometers attached to the crown of the tunnels were used to measure the uplift response of the tunnels.

## CENTRIFUGE TESTING

### Model Preparation

All the models were prepared to the relative density ($D_R$) of approximately 45% using the sand pluviation method with the automatic sand pourer. Hostun sand was used in the models. The material properties are described in Table 2. In the midst of sand pouring, instruments were placed at specific pre-determined depths and locations based on the configuration layout shown in Fig. 2. Tunnels were buried at a depth of 1.1 and 1.5 times of its diameter in the sand to ascertain their difference in floatation response with respect to their depth. Securing supports were also put in place so as to avoid any accidental movement of the tunnels prior to centrifuge testing. After the sand pouring was completed, these sands were saturated with high viscous methyl cellulose fluid prepared at the desired centistokes (cSt) equivalent to the centrifuge g-level. A summary of the test configurations is shown in Table 3.

Methyl cellulose fluid was prepared with a mixture of Hydroxypropyl methylcellulose (HPMC) powder and water. Past studies by Stewart et al (1998) have determined that a desired viscosity at 20 degrees Celsius can be achieved by the following formula:

$$v_{20} = 6.92\ C^{2.54} \qquad \text{(Eq. 1)}$$

where $v_{20}$ is the fluid viscosity at 20 degrees Celsius, and $C$ is the concentration of HPMC in percent.

The methyl cellulose is chemically inert to the constitutive properties of granular soils and produces equivalent peak excess pore pressure as compared to water. In addition, the fluid is also capable of sustaining high pore pressure for liquefaction studies.

### Test Procedure

After model preparation was completed, the centrifuge model package accompanied with the SAM actuator was loaded in one arm of the beam centrifuge, while the other arm was being loaded with an equivalent counterweight. Instrumentation wires were then connected to junction boxes. The connection link of these instrumentations to the computer in the control room was then checked prior to the start of the centrifuge flight.

During the initial 10g acceleration stage, both the centrifuge package and counterweights were swung-up to the horizontal plane. Subsequently, the centrifuge was spun up at intervals of 10g till the desired g-level. An earthquake of predetermined frequency and lever arm offset was then fired. Throughout the centrifuge testing, data were acquired via the Centrifuge Data Acquisition System (CDAQS) and transferred to the computer in the control room. After all planned earthquakes have been fired, the centrifuge was slowed and brought to a halt. The tested centrifuge model was then visually examined for any leads on the floatation failure.

After the centrifuge test, the model was left to drain the methyl cellulose fluid. Once considerable fluid has been removed, excavation of the model will take place to check for any significant movements of the instruments occurred during the test. Other details such as surface upheaval, unexpected fracturing or opening voids within the soil mass were noted.

Table 2. Material properties of Hostun sand

| Properties | Values |
|---|---|
| $\Phi_{crit}$ * | $33^o$ |
| $D_{10}$ | 0.209 mm |
| $D_{50}$ | 0.335 mm |
| $D_{60}$ | 0.365 mm |
| $e_{min}$ * | 0.555 |
| $e_{max}$ * | 1.01 |
| $G_s$ * | 2.65 |

* after Mitrani (2006)

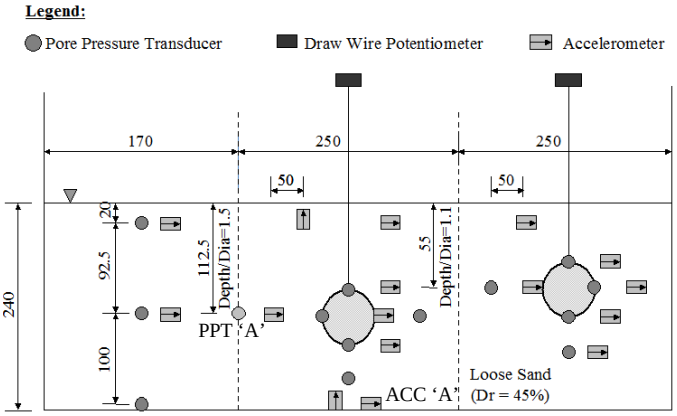


*Fig. 2. Layout of instruments in centrifuge model, NTS*

Table 3: Configurations of centrifuge test

| Description | Configuration |
|---|---|
| Prototype Tunnel Diameter | 5 m |
| Prototype Buried Depth | 7.5 m (1.5 x Dia.) and 5.5m (1.1 Dia.) |
| Relative Density | 45% |
| Type of Soil | Hostun Sand |

## CENTRIFUGE TEST RESULTS

### Initiation and Cessation of Tunnel Floatation

Tunnels generally have a lower unit weight than the surrounding soil. Submerged in saturated soil, these tunnels have a buoyant force which encourages the tunnel to float. However, the overlying weight and shear strength of the overlying soil inhibits the floatation. In the event of liquefaction, the soil loses most of its shear strength and the tunnel may float if the effective buoyant force is greater than the overlying soil weight as expressed in Eq. 2.

$$F_B > F_{WS} + F_{SP} \qquad \text{(Eq. 2)}$$

where $F_B$ is the effective buoyant force after subtracting the weight of the tunnel, $F_{WS}$ is the force due to the weight of the overlying soil, and $F_{SP}$ is the force contribution from the shear planes in the soil. Figure 3 illustrates the above force components.

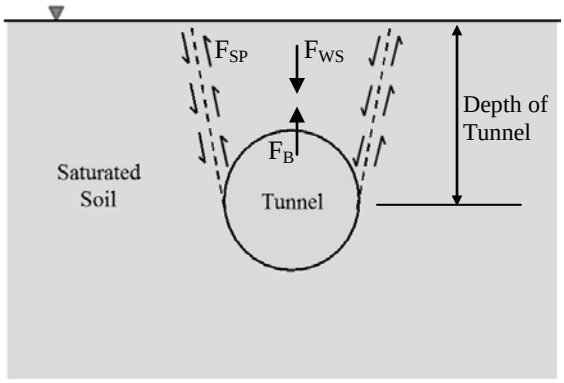


*Fig. 3. Force components acting on tunnel in static condition*

Both tunnels floated with significant uplift displacements. Figure 4 presents the typical floatation trend during cyclic earthquake loading. It is evident that there was an increase in pore pressure immediately with the onset of the cyclic loading. However, the floatation of tunnel took place only in the second cycle of the earthquake.

Due to the uplift tendency of the tunnel, the soil at the crown of the tunnel experienced an increase in vertical stress. As a result, the soil immediately above the tunnel was capable of regaining some of its strength arising from an increase in the effective stress. Time was therefore necessary to overcome this resistance before the tunnel was capable of displacing upwards to the surface. The second factor was due to the time needed for the build up of high excess pore pressure.

Another aspect of floatation can also be observed from the figure. The floatation of the tunnel took place only during the earthquake loading. In addition, the floatation ceased immediately when the loading stopped, despite retaining high excess pore pressures. Clearly, these findings portrayed that the initiation and cessation of tunnel floatation were highly dominated by the earthquake loading rather than the presence of high excess pore pressure alone. The decreasing rate of uplift displacement also signified that the floatation is highly influenced by the sudden application of loading from a static to dynamic condition.

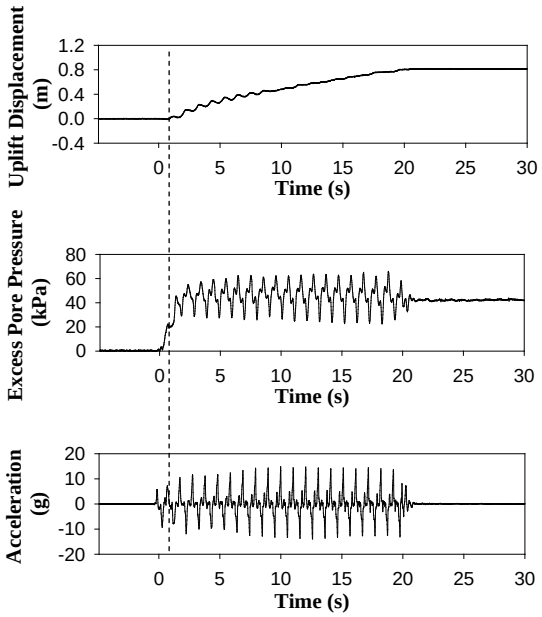


*Fig. 4. Floatation of tunnel accompanied with excess pore pressure (at PPT 'A') and base acceleration (at ACC 'A')*

### Influence of Tunnel Depth

Based on Eq. 2, the depth of a tunnel is a key factor governing the extent of its floatation. A deeper tunnel has a greater overlying soil weight which inhibits floatation. Hence, a shallow buried structure would be more vulnerable to floatation given the lower static weight of the overlying soil inhibiting its uplift throughout the earthquake loading. This is confirmed with larger uplift displacements of shallower tunnels as demonstrated in Fig. 5.

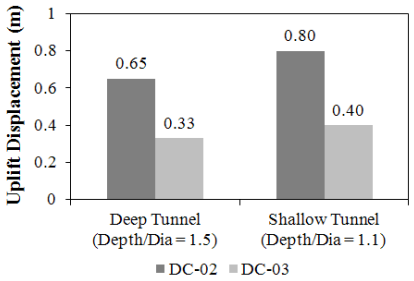


*Fig. 5. Uplift displacements of deep and shallow tunnels*

## CONCLUSION

The centrifuge testing has evidently demonstrated that buried structures do suffer from floatation in the event of

earthquakes. The centrifuge test data has also shown that floatation of tunnels takes place only during the earthquake loading. Furthermore, the initiation of floatation has been found to be highly influenced by the sudden application of cyclic loading from static to dynamic condition. The test data also confirmed that a shallow tunnel is more vulnerable to floatation than a deep tunnel. This is largely due to the lower overburden stress of soil above the tunnel.

REFERENCES


Bardet, J.P., F. Oka, M. Sugito and A. Yashima [1995]. "The Great Hanshin Earthquake Disaster (The 1995 South Hyogo Prefecture Earthquake)", *Preliminary Investigation Report*, Gifu University, Japan.

Bardet, J.P. and C.A. Davis [1999]. "Responses of Large-Diameter Buried Pipes to Earthquakes", *Earthquake Geotechnical Engineering*, (Seco e Pinto, ed.), Rotterdam, pp. 973-986.

Chian, S.C., M.E. Stringer and S.P.G. Madabhushi [2009]. "Use of Automatic Sand Pourer for Loose Sand Models", Submitted to the *Int. Conf. On Physical Modelling in Geotechnics*, Zurich.

Earthquake Engineering Research Institute (EERI) [1994]. "Northridge Earthquake", *Preliminary Reconnaissance Report*, Oak-land, California.

Earthquake Engineering Research Institute (EERI) [1995]. "Northridge Earthquake", *Reconnaissance Report*, Earthquake Spectra, Supplement C to Vol. 11, Vol 1.

Hall, W.J. and T.D. O'Rourke [1991]. "Seismic Behavior and Vulnerability of Pipelines", *Lifeline Earthquake Engineering*, (M.A. Cassaro, ed.), ASCE, New York, pp. 761-773.

Madabhushi, S.P.G., N.E. Houghton and S.K. Haigh [2006]. "A New Automatic Sand Pourer for Model Preparation at University of Cambridge", *Proc. Int. Conf. On Physical Modelling in Geotechnics*, Hong Kong, pp 217-222.

Madabhushi, S.P.G., A.N. Schofield and S. Lesley [1998]. "A New Stored Angular Momentum Based Earthquake Actuator", *Proc. Centrifuge '98*, Tokyo, Vol. 1, pp. 111-116.

Schofield, A.N. [1980]. "Cambridge Geotechnical Centrifuge operations", *Geotechnique*, Vol. 25, No. 4, pp. 743-761.

Schofield, A.N. [1981]. "Dynamic and Earthquake Geotechnical Centrifuge Modeling", *Proc. Int. Conf. on Recent Advances in Geotechnical Earthquake Engineering and Soil Dynamics*, St Louis, Vol. III, pp. 1081-1100.

Seed, H.B. [1970]. "Soil Problems and Soil Behaviour", in *Earthquake Engineering*, Chapter 10, (R.L. Wiegel, ed.), Prentice-Hall, Englewood Cliffs, New Jersey, pp. 227-252.

Stewart, D.P., Y.R. Chen and B.L. Kutter [1998]. "Experience with the Use of Methylcellulose as a Viscous Pore Fluid in Centrifuge Models", *Geotechnical Testing Journal*, Vol. 21, No. 4, pp. 365-369.

Stringer, M.E. and S.P.G. Madabhushi [2009]. "Novel computer controlled saturation of dynamic centrifuge models using high viscosity fluids", ASTM Geotechnical Testing Journal (Paper accepted).

Youd, T.L. and S.N. Hoose [1976]. "Liquefaction During 1906 San Francisco Earthquake", *ASCE Journal of Geotechnical Engineering Division*, Vol. 102, No. GT5, pp. 425-439.

Zhao, Y., K. Gafar, M.Z.E.B. Elshafie, A.D. Deeks, J.A. Knappett and S.P.G. Madabhushi [2006]. "Calibration and use of a new automatic sand pourer", *Proc. Int. Conf. On Physical Modelling in Geotechnics*, Hong Kong, pp 265-270.